

Experiment overview from STAR

Sooraj Radhakrishnan^{1,*} for the STAR Collaboration

¹Kent State University, Kent, OH

Abstract. The STAR experiment at RHIC has a rich experimental program, thanks to the unique datasets covering a wide range of collision energies and collision systems. In this contribution to the proceedings for 2025 Quark Matter conference, we highlight the recent results from STAR, presented in 21 talks and 55 posters. The results presented range from studies of the QCD phase structure and properties of the Quark Gluon Plasma to baryon interactions and nuclear structure

1 Introduction

This year marks the 25th year of data taking by STAR experiment at RHIC. STAR has recently completed (2019 - 2021) data taking for the second phase of the Beam Energy Scan program (BES-II), collecting high statistics datasets of Au+Au collisions covering $\sqrt{s_{NN}} = 3 - 19.6$ GeV (baryochemical potential $\mu_B \sim 760 - 200$ MeV [1]), as shown in Figure 1. STAR operated in a fixed-target mode to allow data taking at lower collision energies, extending reach below $\sqrt{s_{NN}} = 7.7$ GeV. STAR had also recently collected high statistics datasets for Ru+Ru and Zr+Zr (isobar) collisions (2018), O+O collisions and d+Au collisions (2021) at $\sqrt{s_{NN}} = 200$ GeV, in addition to datasets of Au+Au collisions at $\sqrt{s_{NN}} = 27 - 200$ GeV, $p+p$, $p+Au$, $d+Au$, $^3\text{He}+Au$, U+U and several other collision systems at top RHIC energies over the years. These datasets provide a unique opportunity for STAR to study the properties of the Quark Gluon Plasma (QGP) and their collision system dependence, carry out precision measurements to explore the phase structure of QCD matter and study baryon-baryon and baryon-hyperon interactions, bound states and investigate nuclear and hadron structure. Over the past 25 years, STAR has also completed several targeted detector upgrades to better serve the physics goals. The latest being the upgrades for BES-II and the forward upgrades for the data taking in 2022 - 2025 [2]. In these proceedings we highlight some of the recent results presented by STAR at the 2025 Quark Matter (QM) conference.

2 Search for QCD critical point and onset of deconfinement

At high temperatures and $\mu_B \sim 0$, the nuclear matter undergoes a cross-over to the QGP phase. At finite μ_B , model calculations predict it could be a first order phase transition [3]. A key focus of the BES-II program is to search for signals of the possible critical end-point of transition and the QCD phase structure at finite μ_B .

Cumulants of net-baryon number distributions are expected to be sensitive probes of critical dynamics, as the ratio of these cumulants relate directly to the ratios of thermodynamic

*e-mail: skradhakrishnan@lbl.gov

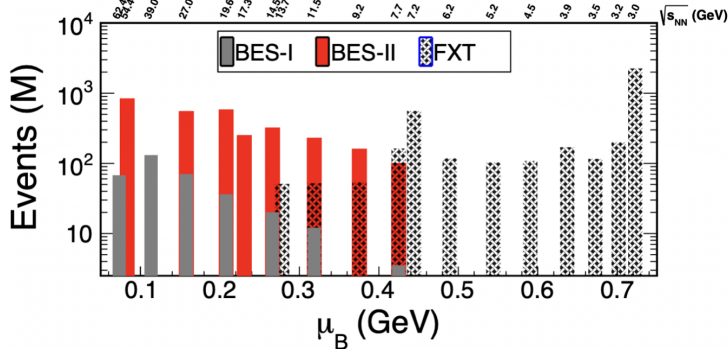


Figure 1. The collision energies and event statistics from STAR BES-II (red and dotted columns) compared to the number of events collected from BES-I (gray columns).

number susceptibilities. STAR has presented precision measurements of cumulants (C_n) up to sixth order and factorial cumulants (κ_n) up to fourth order of net-proton (proxy for net-baryon) distributions in Au+Au collisions at $\sqrt{s_{NN}} = 7.7 - 19.6$ GeV from BES-II at this QM. The measurements in most central 0-5% collisions of the cumulant ratio C_4/C_2 show a deviation of $2 - 5 \sigma$ from models without critical point and from measurements in peripheral (70-80%) collisions at $\sqrt{s_{NN}} = 19.6$ GeV. The results for cumulants and cumulant ratios up to fourth order are now published [4]. STAR had also released at this QM the final results for measurements of proton cumulants, factorial cumulants and their ratios up-to-fourth order in the high μ_B region, from FXT collisions, at $\sqrt{s_{NN}} = 3.2, 3.5$ and 3.9 GeV [5]. The paper detailing the analysis and results is in preparation.

In addition, preliminary results on the rapidity (y) and transverse momentum (p_T) acceptance window dependence of net-proton cumulants in $\sqrt{s_{NN}} = 7.7 - 19.6$ GeV from BES-II were presented [6]. The signals from critical dynamics are expected to increase as the acceptance window are widened. The results show most deviation for the cumulant ratios from UrQMD calculations near 19.6 GeV and in wide acceptance windows. A finite size scaling analysis and Binder cumulant evaluation were performed, following [7], using the rapidity acceptance dependent measurements. These calculations indicate an interesting region in μ_B between 550 - 650 MeV, where possible critical point could be, and warrants further investigations in the high μ_B region.

Baryon-strangeness correlations (C_{BS}) are proposed as a sensitive probe of deconfinement. Detailed correction procedures for C_{BS} measurements, including purity, centrality bin width and efficiency correction for measurements in Au+Au collisions from STAR BES, were presented. These allow precise and reliable C_{BS} measurements to explore the QCD phase diagram [8].

Anisotropic flow is a valuable tool to understand the expansion dynamics and Equation of State (EoS) of the matter produced in heavy-ion collisions. Measurements of elliptic flow v_2 and directed flow v_1 of identified hadrons were presented in Au+Au collisions at $\sqrt{s_{NN}} = 3.0 - 4.5$ GeV from STAR BES-II. Number of Constituent Quark (NCQ) scaling of v_2 , attributed to partonic degrees of freedom, was found to break completely for Au+Au collisions at $\sqrt{s_{NN}} = 3.2$ GeV and below and a gradual restoration was observed towards 4.5 GeV. Hadronic transport models with baryonic meanfield interactions were found to better describe the data at 3.0 GeV in contrast to the data from 4.5 GeV, where partonic transport model AMPT with

string melting was found to give a better description. The measurements indicate an onset of partonic collectivity in the region $\sqrt{s_{NN}} = 3.2 - 4.5$ GeV [9, 10].

Directed flow (v_1) of various identified hadrons was also measured and new preliminary results were shown for Au+Au collisions at $\sqrt{s_{NN}} = 3.2 - 4.5$ GeV from STAR BES-II. Net-kaons were found to show a sign change of the slope, $dv_1/dy|_{y=0}$, from negative v_1 to positive in the collision energy range 4.5 – 7.7 GeV, similar to that of net-protons that showed sign change at a higher collision energy (11.5 – 14.5 GeV). Another significant observation is that of unexpectedly large v_1 measured for ϕ mesons in $\sqrt{s_{NN}} = 3.0 - 4.5$ GeV. The ϕ mesons with a small hadronic scattering cross-section was found to have consistent v_1 as that of protons and Λ , and significantly larger values than for the mesons (pions and kaons) [9].

Measurements of identical charged pion femtoscopic correlations can provide understanding on the geometry of the collision zone at freeze-out, final state interactions and isospin contribution to the EoS. Identical charged pion femtoscopic correlation measurements were presented for $\sqrt{s_{NN}} = 3.0, 3.2, 3.5, 3.9, 4.5, 5.2,$ and 7.7 GeV Au + Au collisions by STAR from BES-II. An estimate of the residual third-body Coulomb effect, utilizing UrQMD to calculate the momentum shift from the effective residual Coulomb charge in the system, was performed. Most of the difference between $\pi^+\pi^+$ and $\pi^-\pi^-$ correlations could be attributed to the residual third-body Coulomb effect, indicating the isospin contribution is likely small [11].

Strange hadron yields and yield ratios can be a valuable probe of deconfinement and EoS of the matter. Measurements of yields and yield ratios of various strange hadrons in Au + Au collisions at $\sqrt{s_{NN}} = 3.2, 3.5, 3.9, 4.5, 5.2$ and 6.2 GeV from BES-II were presented. The Λ/K_S^0 yield ratio was studied as a function of collision centrality. An enhancement of the Λ/K_S^0 yield ratio in central collisions, relative to peripheral, for $p_T > 1$ GeV/c was observed for collision energies $\sqrt{s_{NN}} > 3.9$ GeV. An enhancement of the baryon to meson ratio in central heavy-ion collisions at higher collision energies is typically attributed to coalescence hadronization from a deconfined medium. The current observation along with model studies could help probe the onset of deconfinement as a function of collision energy [12].

3 QGP properties and emergent phenomena

3.1 Search for QGP in small systems

The origin of the observed azimuthal anisotropies in small collision systems and whether they arise from collective medium response, is one of the questions of major focus currently in high energy nuclear physics. The recent STAR O+O and d +Au datasets at $\sqrt{s_{NN}} = 200$ GeV allows for an effective geometry scan at RHIC. The multiplicity range are comparable between O+O and d +Au collisions. However, the second order eccentricity (ϵ_2) is much larger in d +Au compared to O+O collisions. The measured v_2 values show the same ordering, with the values in d +Au much larger than in O+O collisions in high multiplicity event classes. The v_2 and v_3 values after peripheral subtraction shows consistent values between the two systems as a function of multiplicity, once scaled by ϵ_2 and ϵ_3 , respectively, calculated using sub-nucleon Glauber. These observations indicate origin of v_n from medium response to initial geometry in these collisions [13].

A signature of QGP formation in heavy-ion collisions is the energy loss and suppression of hard probes, evidence to which were so far lacking in small collision systems. With the O+O dataset, STAR has presented new preliminary results of nuclear modification factors R_{AA} , R_{CP} and I_{CP} at this QM. Measurements of inclusive charged hadron R_{AA} and R_{CP} at high p_T , inclusive jet R_{CP} , and semi-inclusive hadron+jet I_{CP} in O+O collisions at $\sqrt{s_{NN}} = 200$ GeV were presented [14]. Inclusive charged hadron and jet R_{CP} and h+jet I_{CP} are found

to be below unity, showing suppression of yields in central collisions relative to peripheral collisions. Further studies on effects other than jet quenching from QGP that can give rise to this suppression, including understanding of potential bias in peripheral event class, are required to make conclusions on evidence of jet quenching in O+O collisions at RHIC.

Measurement of strangeness production and yield ratios of strange hadrons in O+O collisions were also presented. Measured yield ratio of Ω baryons to ϕ mesons show an enhancement in central O+O collisions, compared to $p+p$ collisions, at $\sqrt{s_{NN}} = 200$ GeV. The enhancement observed in central O+O collisions is consistent with that observed in Ru+Ru/Zr+Zr collisions at similar number of participants [15].

3.2 Constraining QGP properties

Results on thermal dielectron measurements in Au+Au collisions at $\sqrt{s_{NN}} = 7.7 - 54.4$ GeV were presented. Temperature values were extracted from the dielectron invariant mass spectra in the intermediate mass region (IMR) at 54.4 and 27 GeV and low mass region (LMR) at 14.6, 19.6, 27 and 54.4 GeV and were presented. The dielectron emission in the IMR mass region ($1.0 < M_{ee} < 2.9$ GeV/c²) is dominated by QGP thermal radiation while the dielectrons in the low mass region ($0.4 < M_{ee} < 1.2$ GeV/c²) are emitted at later stages, closer to the transition to hadrons. The extracted temperature values from LMR are consistent with the expected pseudo critical temperature at these energies, while those from the IMR are much higher, consistent with emission from a QGP phase [16]. A higher precision extraction of the temperatures in the LMR and IMR from isobar (Ru+Ru, Zr+Zr) collisions at $\sqrt{s_{NN}} = 200$ GeV were also presented [17].

Direct virtual photon yields, dN_γ/dy , measured as a function of charged particle multiplicity at mid-rapidity, $dN_{ch}/d\eta$, were shown for collision energies from $\sqrt{s_{NN}} = 14.6 - 200$ GeV [18]. All the STAR measurements from $\sqrt{s_{NN}} = 14.6 - 200$ GeV were found to follow a common power-law dependence, $dN_\gamma/dy = AdN_{ch}/d\eta^\alpha$, with $\alpha = 1.43 \pm 0.04$ (stat) ± 0.04 (sys), indicating a similar origin to the direct photon yields across these energies.

Preliminary results on precision measurement of Λ and $\bar{\Lambda}$ hyperon global polarization from BES-II in Au+Au collisions at $\sqrt{s_{NN}} = 7.7 - 17.3$ GeV were presented. The polarization measured for both Λ and $\bar{\Lambda}$ are consistent within uncertainties and no indication of splitting induced by magnetic field B is observed. The measurement helps put constraint on the late stage B field in the collisions. New preliminary measurements of global polarization of multi-strange hyperons Ξ and Ω were also presented. The Ξ hyperon polarization was measured to be consistent with that of Λ within uncertainties while Ω showed hints of larger values, albeit with large uncertainties [19].

Studies searching for signals from a possible chiral magnetic wave (CMW) in heavy-ion collisions were presented. In particular, measurement of the CMW sensitive observable ΔC - covariance between charge dependant elliptic flow and charge asymmetry in the system - was made for the two isobar collision species, Ru+Ru and Zr+Zr at $\sqrt{s_{NN}} = 200$ GeV. No enhancement of the observable in Ru+Ru collisions compared to Zr+Zr collisions was observed, despite the former having four additional protons and thus larger magnetic field and potential CMW [20].

Measurement of baryon to meson ratio within jets was performed. The preliminary results presented show no significant modification of p/π yield ratio within jets between $p+p$ and Au+Au collisions at $\sqrt{s_{NN}} = 200$ GeV. This contrasts with the inclusive measurements which show strong enhancement in Au+Au compared to that in $p+p$, and commonly attributed to radial flow and coalescence hadronization in heavy-ion collisions. The ratios also show no in cone radial evolution of the ratios within jets [21].

Constraining the contribution from hadronic interactions to anisotropic flow observables, after freeze-out from the QGP phase, is important for using them to understand QGP properties. New preliminary results on measurement of v_1 of K^{*0} resonance in Au+Au collisions at $\sqrt{s_{NN}} = 14.6, 19.6$ and 27 GeV were presented. The v_1 of K^{*0} show a sign change with centrality, unlike that of charged kaons. Hydrodynamic calculations with a hadronic afterburner was able to describe the centrality dependence, while hydrodynamic calculations without hadronic afterburner failed to. The measurements show v_1 of K^{*0} as an attractive probe to constrain late stage hadronic interactions [22].

The colliding heavy-ions act as a source of quasi-real photons that are linearly polarized along the impact parameter direction. Polarization of photo-produced J/ψ are measured relative to the reaction plane (impact parameter direction). The J/ψ are found to be strongly polarized along the reaction plane with polarization values independent of centrality. The measurement also opens up the possibility of using photo-produced J/ψ polarization as a tool to determine the reaction plane direction in peripheral and ultra peripheral collisions [23].

4 Baryon interactions and nuclear structure

Femtoscopic correlations are a powerful tool to study final state interactions among the particles produced in heavy-ion collisions. Nucleon - hyperon (NY) interactions can be studied through femtoscopic correlations and provides an alternate way to search for the existence of strange dibaryons. Preliminary results on measurements of femtoscopic correlation functions and extracted strong interaction parameters - scattering length f_0 and effective range d_0 - using Lednicky-Lyuboshitz fits to the correlation functions for $p - \Xi^-$ and $p - \Omega^-$ correlations from Ru+Ru and Zr+Zr collisions at $\sqrt{s_{NN}} = 200$ GeV were presented. The extracted f_0 was found to be negative for $p - \Omega^-$ correlations, providing evidence for the existence of a strange dibaryon bound state. For $p - \Xi^-$, the extracted f_0 was positive [24].

Nucleon - hyperon femtoscopic correlations can also be used to study hypernuclei. An extraction of the hypertriton ($^3_{\Lambda}H$) binding energy (BE) using f_0 and d_0 from the measured d- Λ correlations was presented. New preliminary measurements with Au+Au collisions at $\sqrt{s_{NN}} = 3.0$ GeV from Run 21 provides the BE as $0.06+0.06-0.02$ MeV/ c^2 for the hypertriton, making it the most precise extraction of hypertriton BE. New preliminary measurements of t- Λ and $^3\text{He}-\Lambda$ correlation functions were also presented [25].

New preliminary measurements of yields of various hypernuclei ($^3_{\Lambda}H$, $^4_{\Lambda}H$, $^4_{\Lambda}He$, $^5_{\Lambda}He$) in Au+Au collisions at different BES-II energies were presented. The thermal model was found to generally over-predict the yields of the hypernuclei in these collisions. The measurements provide insight into the production mechanism of light hypernuclei in heavy-ion collisions [26].

In addition to studying light nuclei, heavy-ion collisions can also be used as a valuable tool to image the shape of heavier nuclei. Anisotropic flow (v_n), p_T and v_n fluctuations and their correlations carry information about the initial conditions and thus the shape of the colliding nuclei. Ratios of measurements of these quantities in U+U collisions at $\sqrt{s_{NN}} = 193$ GeV and Au+Au collisions at $\sqrt{s_{NN}} = 200$ GeV were systematically compared to hydrodynamic model calculations to extract constraints on the shape parameters of U nuclei and were presented, along with potential applications of this approach for future research [27].

Preliminary results from a new measurement, looking into the spin correlation of Λ and $\bar{\Lambda}$ pairs were also presented. The measurements can shed light into the spin correlation of $s\bar{s}$ pairs and how these correlations are modified through hadronization [28].

5 Summary and Outlook

STAR has presented new results at this conference that significantly advance our understanding of the QCD phase structure, QGP properties, light nuclei bound states, baryon - hyperon interactions, spin correlations and nuclear structure. STAR's science mission continues with a focus to complete analysis of BES-II data, and analysis of the high statistics $p+p$, Au+Au and possibly p +Au datasets at $\sqrt{s_{NN}} = 200$ GeV collected in 2022 – 2025 with a focus on forward physics and complementarity to EIC and probing QGP's microstructure using hard probes.

References

- [1] A. Andronic, P. Braun-Munzinger, J. Stachel, Nucl. Phys. A **772**, 167-199 (2006). <https://doi.org/10.1016/j.nuclphysa.2006.03.012>
- [2] Q. Yang for the STAR Collaboration, Nucl. Phys. A **982**, 951-954 (2019). <https://doi.org/10.1016/j.nuclphysa.2018.10.029>
- [3] M. A. Stephanov, Int.J.Mod.Phys. **A20**, 4387-4392 (2005)
- [4] B. E. Aboona et al. (STAR Collaboration), Phys. Rev. Lett. **135**, 142301 (2025) <https://doi.org/10.1103/9l69-2d7p>
- [5] Z. Sweger for the STAR Collaboration, Talk at Quark Matter 2025, Contribution ID 872
- [6] Y. Huang for the STAR Collaboration, This proceedings
- [7] A. Sorensen, P. Sorensen, arXiv:2405.10278 <https://doi.org/10.48550/arXiv.2405.10278>
- [8] H. Feng for the STAR Collaboration, This proceedings
- [9] S. Sharma for the STAR Collaboration, This proceedings
- [10] B. E. Aboona et al. (STAR Collaboration), Phys. Rev. Lett. **135**, 072301 (2025) <https://doi.org/10.1103/2qhx-cp79>
- [11] V. Luong for the STAR Collaboration, This proceedings
- [12] H. Li for the STAR Collaboration, This proceedings
- [13] Z. Yan for the STAR Collaboration, This proceedings; STAR Collaboration, arXiv:2510.19645 <https://doi.org/10.48550/arXiv.2510.19645>
- [14] S. Zhang for the STAR Collaboration, This proceedings
- [15] W. Yuan for the STAR Collaboration, This proceedings
- [16] B. E. Aboona et al. (STAR Collaboration), Nature Communications **16**, 9098 (2025) <https://doi.org/10.1038/s41467-025-63216-5>
- [17] J. Luo for the STAR Collaboration, Talk at Quark Matter 2025, Contribution ID 918
- [18] X. Bao for the STAR Collaboration, This proceedings
- [19] T. Lu for the STAR Collaboration, This proceedings
- [20] A. Nain for the STAR Collaboration, This proceedings
- [21] G. Del Gau for the STAR Collaboration, This proceedings
- [22] Md. Nasim for the STAR Collaboration, This proceedings
- [23] K. Wang for the STAR Collaboration, This proceedings
- [24] K. Zhang for the STAR Collaboration, This proceedings
- [25] X. Jiang for the STAR Collaboration, This proceedings
- [26] Y. Zhou for the STAR Collaboration, This proceedings
- [27] C. Zhang for the STAR Collaboration, This proceedings
- [28] B. E. Aboona et al. (STAR Collaboration), Nature **650** 65 (2026) <https://doi.org/10.48550/arXiv.2506.05499>